
COVERAGE-GUARANTEED SPEECH EMOTION RECOGNITION VIA CALIBRATED UNCERTAINTY-ADAPTIVE PREDICTION SETS

A PREPRINT

 **Zijun Jia**

School of Automation Science and Electrical Engineering
Beihang University
Beijing, 100191, China
21375166@buaa.edu.cn

April 28, 2025

ABSTRACT

Road rage, stemming from emotional suppression and outbursts, can lead to traffic incidents such as rear-end collisions, crashes, and aggressive confrontations, posing significant risks to road safety and public security. Speech Emotion Recognition (SER) methods can detect early signs of negative emotions and provide real-time alerts to drivers, effectively reducing the likelihood of accidents. However, previous studies, such as Hidden Markov Models (HMMs) and Long Short-Term Memory (LSTM) networks, predominantly rely on one-dimensional speech signals, and are prone to overfitting and miscalibration issues, undermining their reliability in high-stakes applications. In this paper, we introduce a risk management framework that produces prediction sets with statistically rigorous guarantees of correctness coverage marginally over the test set. Specifically, we separate a held-out calibration set and develop a binary loss function for each data point to determine whether the ground-truth label is covered by the prediction set, which is calibrated by a data-driven threshold λ . We develop a joint loss function on the calibration set, and given a user-specified risk level α , we then calibrate the threshold λ to strictly bound it such that we can manage the expectation of the loss of each test point by this predefined upper bound α . We conduct extensive evaluations on 6 base models on 2 datasets. Empirical results demonstrate that we can always bound the average correctness coverage rate (i.e., $\geq 1 - \alpha$) at various user-specified risk levels. Moreover, we consistently control the marginal error rate across various splitting ratios (e.g., 0.1) between the calibration and test set, highlighting the robustness and effectiveness of our framework. Furthermore, we propose a small batch online calibration framework based on the local exchangeability assumption, which is suitable for complex scenarios where there is data domain offset or non-IID between batches. By constructing a non-negative test martingale, we ensure the coverage of the prediction set in dynamic scenarios, and verify the effectiveness of this method in controlling the coverage of the prediction set through cross-dataset experiments.

1 Introduction

In recent years, road rage has become an increasingly serious traffic safety problem worldwide. With the acceleration of urbanization and the increase in car ownership, traffic congestion and driving pressure are increasing, resulting in more and more drivers showing extreme emotional reactions while driving. Studies have shown that road rage not only increases the incidence of traffic accidents, but also exacerbates conflicts between drivers and other road users, further threatening public safety. According to the National Highway Traffic Safety Administration, more than one-third of traffic accidents are related to drivers losing control of their emotions, and this proportion is on the rise.

Speech emotion recognition technology, as a means of emotion recognition based on speech signal analysis, has gradually become an effective tool for solving problems such as road rage. By capturing the driver's voice characteristics in real time and analyzing his or her emotional state, speech emotion recognition can provide timely emotional feedback to the

traffic management system, helping to predict and intervene in potential dangerous driving behaviors. This technology can not only provide more accurate emotion monitoring in smart cars, but can also be applied to other emotion-related fields, such as customer service and mental health monitoring. Therefore, the importance of speech emotion recognition is increasing day by day, becoming one of the core research directions in the fields of intelligent transportation systems, unmanned driving technology, and emotion analysis.

With the rapid development of deep learning technology, speech emotion recognition tasks based on convolutional neural networks have made significant progress. This paper extracts the Mel-spectrogram features of speech signals to characterize different emotion categories and conducts experimental comparisons. Despite this, the model may still encounter overfitting problems during training, resulting in performance degradation on new and unseen data. In addition, current deep learning models generally lack confidence or uncertainty measures for prediction results, which means that in practical applications, the model's predictions may be unreliable. Recent studies have pointed out that the miscalibration problem still exists. For example, Zhao et al. (2023) pointed out that although convolutional neural networks show high accuracy in speech emotion recognition tasks, the confidence scores of their prediction results are often too high and fail to truly reflect the actual performance of the model, resulting in incorrect emotion recognition. Therefore, improving the uncertainty measure of the model has become the key to improving the performance of speech emotion recognition systems Psaros et al. [2023], Wang et al. [2025a].

To solve these problems, the conformal prediction method provides a new solution. CP can not only give a predicted label, but also build a set of all possible prediction results and provide a confidence guarantee for each prediction result. To ensure that the confidence of the selected label meets the risk tolerance specified by the user, specifically, the Mel-spectrogram feature is used as the feature extraction method in the speech emotion recognition task, and 5 neural networks with basically the same parameter quantity are trained on the IEMOCAP dataset to obtain a pre-trained model. After the feature extraction and model training are completed, the Conformal Prediction framework is used to evaluate the model to ensure the reliability of the prediction results. Specifically, by defining non-conformal scores and associating these scores with the real emotion labels, the calibration set is used to calibrate the model. In this process, the test data is processed according to the risk level (alpha value) specified by the user, and finally a prediction set with marginal coverage guarantee is generated. This process ensures that the emotion recognition model not only gives the emotion label, but also provides a confidence estimate for the label, thereby ensuring the statistical reliability of the prediction results.

Although CP can effectively provide coverage guarantee, it only solves the coverage problem of the prediction set without considering the reliability of the model under different risk levels. In order to solve this problem, a risk control framework is further introduced. The core idea of this framework is to adjust the risk level of the model on the basis of maintaining coverage guarantee to cope with various uncertainties that may arise in practical applications. Under the risk control framework, the beta value is used to quickly determine the optimal prediction set size through binary search. By processing the calibration set, the size of the prediction set can be adjusted under the constraint of a given risk level to meet the needs of risk control. At the same time, the loss function has been improved so that it not only focuses on the prediction error rate, but also considers the size of each prediction set and its uncertainty. The improvement of the loss function enables the framework to be flexibly applied to different tasks and scenarios, such as emotion recognition, intelligent traffic monitoring, etc. By combining CP with risk control, not only the coverage of the model is guaranteed, but also the robustness and accuracy of the model are improved, so that it can adapt to different practical application needs. Experimental results show that the framework can achieve coverage guarantee at different risk levels, while reducing the uncertainty of the model to a certain extent, making it more valuable for practical applications. However, traditional CP methods rely on a strict assumption of data exchangeability, which is valid in controlled environments but often fails in dynamic real-world scenarios, such as speech emotion recognition, where the data distribution may change between batches or domains. Such a non-exchangeable environment leads to a degradation of coverage guarantees, thus limiting the practical application of CP. To overcome this limitation, we propose a novel framework to ensure the coverage of the prediction set in dynamic scenarios by performing conformal prediction via a mini-batch online calibration mechanism. Specifically, we relax the global exchangeability assumption by adopting a local exchangeability assumption within a mini-batch. By constructing a non-negative test martingale, our method ensures coverage even when the distribution changes between batches, such as speaker differences or acoustic environment differences.

In order to verify the effectiveness of the framework, a large number of experiments were carried out. First, starting from the pre-experimental part, the performance of different feature selection methods and pre-trained models was tested. In the pre-experimental stage, a variety of feature extraction methods were compared, including mel-spectrogram features, chromaticity features, and spectral contrast features. Through testing on the TESS dataset, it was found that the performance of mel-spectrogram features was better than other feature extraction methods, achieving a test set accuracy of 99.82%. Therefore, mel-spectrogram features were finally selected as the speech feature extraction method. Next, several different neural network models, including ResNet, MobileNetV3, ShuffleNetV2, etc., were trained on the IEMOCAP dataset, and their performance on emotion recognition tasks was tested. Although the accuracy of

these models on the training set reached 100%, the accuracy on the test set dropped to 41.60%, 31.94%, and 34.13%, respectively. This phenomenon indicates that the model has a certain overfitting problem when facing unseen data, so the Conformal Prediction framework is introduced to ensure the reliability and statistical significance of the model prediction results. In order to prove the coverage guarantee of the framework, two rounds of verification were carried out. The first round of experiments was conducted on the same dataset to ensure that the model can provide stable performance on both the calibration set and the test set, verifying that Conformal Prediction can guarantee the accuracy of the prediction results under a given risk level. The second round of experiments conducted cross-dataset validation, that is, the model trained on the IEMOCAP dataset was applied to the TESS dataset to test the generalization ability of the model. The experimental results show that the model can still maintain a high coverage on different datasets and can effectively adapt to different data distributions, verifying the robustness of the framework. Next, the uncertainty of different models is evaluated based on the prediction set size. During the training and testing process of each model, the prediction set size is calculated, and the uncertainty of the model is quantified according to the prediction set size under each alpha value. By conducting multiple experiments under approximately the same parameter conditions, we found that when the uncertainty of the model increases, the prediction set size usually increases. This shows that a larger prediction set means that the model has lower confidence in the recognition of certain emotion categories. To control this uncertainty, we adopt the risk control framework to conduct the same experiment, and combine it with the improved loss function to optimize the prediction set size to ensure that the model can provide reliable prediction results under different risk levels. The final experimental results show that both frameworks can maintain the coverage guarantee and robustness of the final results under different datasets and risk levels, ensuring that the emotion recognition system can meet the needs of practical applications. Crucially, to verify our small batch martingale value method in the scenario of non-IID and domain shift, we designed an additional experiment in which the calibration and test data come from different datasets (IEMOCAP for calibration and TESS for testing), explicitly violating global exchangeability. The data is split into small batches (5 calibration samples + 1 test sample per batch), and the small amount of data within the batch is assumed to be locally exchangeable, while allowing for distribution shifts across batches. The coverage of traditional CP methods that rely on global exchangeability will drop significantly. In contrast, our martingale-based method brings the coverage close to the theoretical bound. This experiment finally proves the effectiveness of our framework in the scenario of non-IID and domain shift.

2 Related Work

2.1 Speech Recognition

The history of speech recognition technology can be traced back to the 1950s. The initial systems relied on traditional algorithms based on template matching, which usually required users to pronounce in a specific way. With the improvement of computing power, hidden Markov models (HMMs) have become the mainstream technology for speech recognition, which can effectively model speech signals in time series. However, these traditional methods still face problems with recognition accuracy and noise interference, especially in complex speech environments. The performance of traditional speech recognition systems often cannot meet the requirements of high accuracy and high robustness. After entering the era of deep learning, speech recognition technology based on neural networks has completely changed this situation. In particular, the introduction of convolutional neural networks (CNNs) and recurrent neural networks (RNNs) has made the processing of speech signals more efficient and accurate. Technologies such as deep neural networks (DNNs) and long short-term memory networks (LSTMs) have greatly improved the accuracy and real-time performance of speech recognition by automatically extracting features and performing end-to-end training. Today, deep learning has become the core technology of speech recognition and is widely used in smart assistants, speech-to-text, speech translation and other fields. In terms of speech emotion recognition, the advantages of deep learning are also significant. Traditional emotion recognition methods mostly rely on manually extracted features, such as pitch, volume, rhythm, etc. Although they can provide certain information for emotion classification, they are unable to cope with complex emotions. The emotion recognition system based on deep learning, especially in combination with CNN, LSTM and other network structures, can automatically learn richer emotional features from a large amount of speech data, improving the accuracy and robustness of emotion recognition. This has enabled speech emotion recognition to achieve breakthrough progress in multiple application scenarios, especially in the fields of intelligent transportation, customer service, mental health, etc., showing great application potential.

2.2 Conformal Prediction

CP [Angelopoulos and Bates \[2021\]](#), [Ye et al. \[2024\]](#), [Barber et al. \[2023\]](#), [Wang et al. \[2024\]](#), [Sun and Yu \[2023\]](#), [Wang et al. \[2025b\]](#) is an uncertainty quantification method that provides strict statistical guarantees for machine learning models. Unlike traditional point prediction, CP provides a set of possible prediction labels for each input sample, rather than just a single prediction label, by generating a prediction set containing the prediction results. The core

idea is to calculate the nonconformity score to measure the difference between each predicted label and the model’s prediction result, thereby deciding whether the label should be included in the prediction set. The nonconformity score measures the model’s confidence in the prediction result. For classification tasks, it is based on the difference between the model’s predicted probability of the true category and the actual category; for regression tasks, it is the difference between the predicted value and the true value. Before generating the prediction set, Conformal Prediction first uses a calibration set to estimate the distribution of the nonconformity score. The calibration set is a part of the data separated from the training set and is specifically used to measure the prediction uncertainty of the model. By calculating the nonconformity score in the calibration set, Conformal Prediction generates a quantitative value that defines which prediction labels the model should include at a given confidence level. In the test phase, for each new sample, the model outputs a predicted label and its corresponding nonconformity score. Then, CP generates a prediction set by comparing the inconsistency score of each label with the quantized value in the calibration set. The prediction set contains all labels whose inconsistency scores are less than or equal to the quantized value. In this way, the generated prediction set can ensure that the true label always appears in the prediction set at the specified confidence level. This provides a coverage guarantee, that is, at the set confidence level, the probability that the generated prediction set contains the true label is at least the confidence level (such as 90%). This guarantee applies to all models and does not depend on any assumed data distribution, so it is called a distribution-independent prediction method.

3 Method

3.1 Preliminaries

As a statistical consistency prediction method, the Split Conformal Prediction(SCP) framework shows unique advantages in the reliability evaluation of machine learning models by converting heuristic uncertainty measures into prediction sets with strict probability guarantees. Its core idea is based on the assumption of data exchangeability and combines the quantile calibration of nonconformity scores to achieve coverage probability control of unknown samples. The theoretical basis and algorithm flow of SCP will be systematically explained below.

3.1.1 Theoretical Foundations and Algorithm Process

1. Problem Definition and Input Conditions

- **Input Data:**

- Calibration dataset $\{(X_t, Y_t^*)\}_{t=1}^n$, satisfying the independent and identically distributed (i.i.d.) assumption.
- Pretrained classification model $\hat{f}(\cdot)$, with output as a class probability vector $\hat{f}(X_t) \in [0, 1]^K$, where the true label probability is $\hat{f}(X_t)_{Y_t^*}$.

- **Objective Function:** Construct the prediction set $\mathcal{C}(X_{\text{test}})$ such that the coverage probability of the true label satisfies:

$$\mathbb{P}(Y_{\text{test}}^* \in \mathcal{C}(X_{\text{test}})) \geq 1 - \alpha \quad (1)$$

2. Nonconformity Score Definition and Quantile Calibration The nonconformity score s_t reflects the model’s uncertainty in predicting the true label, defined as:

$$s_t = 1 - \hat{f}(X_t)_{Y_t^*} \quad (2)$$

Sort the scores of the calibration set in ascending order: $\{s_1 \leq s_2 \leq \dots \leq s_n\}$, and Get the $\frac{\lceil (n+1)(1-\alpha) \rceil}{n}$ quantile from $\{s_t\}_{t=1}^n$:

$$\hat{q} = \inf \left\{ q : \frac{|\{t : s_t \leq q\}|}{n} \geq \frac{(n+1)(1-\alpha)}{n} \right\} = s_{\frac{\lceil (n+1)(1-\alpha) \rceil}{n}} \quad (3)$$

Key Derivation: Based on the exchangeability assumption, the nonconformity score s_{test} of the test sample is uniformly distributed among the calibration scores in the sorted sequence. The coverage probability strictly satisfies:

$$\mathbb{P}(s_{\text{test}} \leq \hat{q}) = \frac{\lceil (n+1)(1-\alpha) \rceil}{n+1} \geq 1 - \alpha \quad (4)$$

Here, the ceiling function $\lceil \cdot \rceil$ ensures the conservativeness of the threshold, thus guaranteeing the lower bound of the coverage probability.

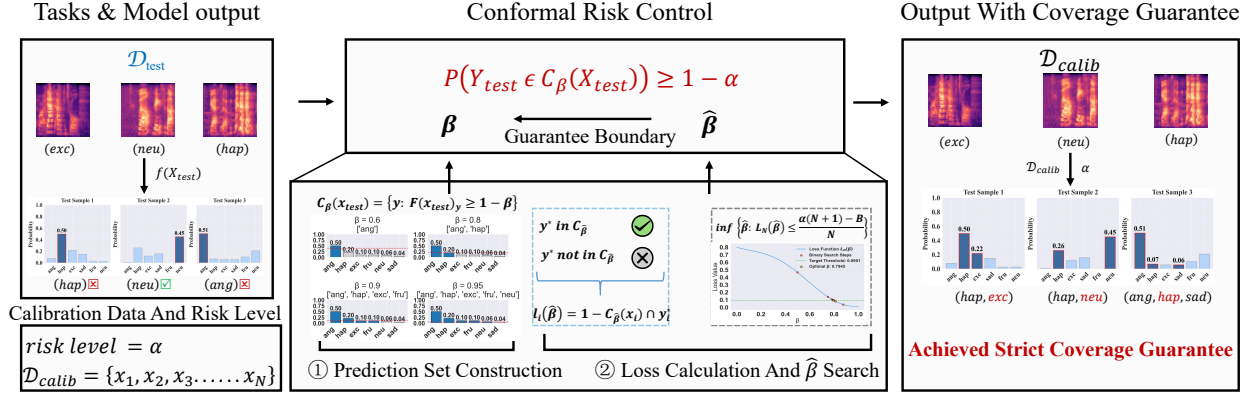


Figure 1: Conformal Risk Control Framework

3. Prediction Set Construction and Coverage Validation For the test sample X_{test} , the prediction set includes all classes satisfying the following condition:

$$\mathcal{C}(X_{\text{test}}) = \left\{ y \in [K] : 1 - \hat{f}(X_{\text{test}})_y \leq \hat{q} \right\} \quad (5)$$

Example Operation:

- If the predicted probability for a class $\hat{f}(X_{\text{test}})_y \geq 1 - \hat{q}$, the class is included in the prediction set.
- The final prediction set size is dynamically adjusted, balancing confidence and classification granularity.

3.1.2 Mathematical Proof Supplement

Theorem (Marginal Coverage Guarantee): Under the data exchangeability assumption, the SCP framework satisfies:

$$\mathbb{P}(Y_{\text{test}}^* \in \mathcal{C}(X_{\text{test}})) \geq 1 - \alpha \quad (6)$$

Proof: Let the combined sequence of calibration and test scores be $s_{(1)} \leq s_{(2)} \leq \dots \leq s_{(n+1)}$, with the rank k of the test score s_{test} following a uniform distribution $k \sim \text{Uniform}\{1, \dots, n+1\}$. Select the threshold $\hat{q} = s_{(k^*)}$, where $k^* = \lceil (n+1)(1 - \alpha) \rceil$, then:

$$\mathbb{P}(s_{\text{test}} \leq \hat{q}) = \mathbb{P}(k \leq k^*) = \frac{k^*}{n+1} \geq 1 - \alpha \quad (7)$$

3.2 Risk Control in speech emotion recognition task1

To adapt the framework of split conformal prediction to the Speech emotion recognition task for user - specified guarantees of task - specific performance, we define a loss function for each calibration data, formulated as

$$l(C(X_t), Y_t) = \mathbf{1}\{Y_t \notin C(X_t)\} \quad (8)$$

Conformal Risk Control (CRC) provides statistical guarantees for high - risk classification tasks through the exchangeable data assumption and custom - defined loss functions. Given N calibration data points and 1 test data point (with a total of K classes), CRC first constructs a prediction set for the sample x_i :

$$C_\beta(x_i) = \{y : F(x_i)_y \geq 1 - \beta\} \quad (9)$$

where $F(x_i)$ is the probability distribution output by the model, and β controls the confidence threshold. The task - specific loss is defined as $l_i = 1 - |C_\beta(x_i) \cap y_i^*|$ (if the true label $y_i^* \notin C_\beta(x_i)$, then $l_i = 1$), and its expectation must satisfy $\mathbb{E}[l_{\text{test}}] \leq \alpha$. Based on data exchangeability, the expectation of the test loss can be expressed as:

$$\mathbb{E}[l_{\text{test}}(\beta)] = \frac{NL_N(\beta) + l_{\text{test}}(\beta)}{N+1} \leq \alpha \quad (10)$$

where $L_N(\beta) = \frac{1}{N} \sum_{i=1}^N l_i$ is the average loss of the calibration set. By solving for the optimal threshold

$$\hat{\beta} = \inf \left\{ \beta : \frac{NL_N(\beta) + B}{N + 1} \leq \alpha \right\} \quad (11)$$

(where B is the task - related loss upper bound, e.g., $B = 1$), $\hat{\beta}$ is determined and applied to the test data to construct $C_{\hat{\beta}}(x_{\text{test}})$, ensuring risk control. This framework flexibly designs loss functions (such as coverage loss $l_i = 1 - \text{coverage}$ or sparsity loss $l_i = |C_{\beta}(x_i)|$), transforming abstract task metrics (like false positive rate and prediction set size) into an optimizable form, thereby achieving task - specific metric guarantee.

3.3 Comparison of two frameworks

Conformal Risk Control has a core drawback compared to Split Conformal Prediction in terms of lower computational efficiency, mainly due to its need for multiple traversals of the calibration data to optimize the threshold. Specifically:

The threshold calculation of SCP only requires a single sorting of the non-conformity scores $s_t = 1 - \hat{f}(X_t)Y_t^*$ on the calibration set, and taking the quantile \hat{q} , with a time complexity of $O(N \log N)$

CRC needs to traverse candidate thresholds β . For each candidate value, it calculates the average loss on the calibration set $L_N(\beta) = \frac{1}{N} \sum_{i=1}^N l_i$, and then verifies the condition $\frac{NL_N(\beta) + B}{N + 1} \leq \alpha$. Assuming the number of candidate β is M , its time complexity is $O(M \cdot N)$. Even with binary search optimization (iteration times $O(\log M)$), it still requires multiple complete traversals of the calibration set, leading to a significant increase in computational load.

This efficiency bottleneck is particularly prominent in large-scale calibration sets ($N \gg 1$) or high-real-time scenarios (such as autonomous driving), while the lightweight single sorting of SCP has more advantages. The flexibility of CRC comes at the cost of efficiency, and one needs to balance the choice according to task requirements.

3.4 Mini-batch conformal prediction theory under non-IID1

In light of the limitations of traditional conformal prediction, which relies on global data exchangeability [Barber et al. \[2023\]](#), [Kang et al. \[2024\]](#), [Wang et al. \[2025c\]](#), we propose the assumption of within - batch local exchangeability. We prove that even when there are differences in data distributions between batches (i.e., batch - to - batch exchangeability may not hold), we can still strictly guarantee the global coverage probability by constructing a non - negative test supermartingale with a forcing operation. This framework breaks through the strong dependence of classical theories on independent and identically distributed data, providing universal theoretical support for small - batch scenarios such as time - series data and online learning.

E - value [Gauthier et al. \[2025\]](#), as a non - negative random variable satisfying $E[E] \leq 1$, can directly construct conformal sets through probability inequalities, offering a more flexible uncertainty quantification tool. For the calibration set $D_{\text{cal}} = \{(X_i, Y_i)\}_{i=1}^n$ and the test sample (X_{n+1}, Y_{n+1}) , the E - value is defined as:

$$E = \frac{S_{n+1}}{\frac{1}{n+1} \sum_{i=1}^{n+1} S_i} \quad (12)$$

where $S_i = S(X_i, Y_i)$ and S is a non - conformity score (such as cross - entropy loss) with non - negative values. Under the assumption of within - batch data exchangeability, the conditional expectation of the E - value satisfies $E[E_t | F_{t-1}] = 1$, which provides a crucial basis for constructing the martingale process.

The filtration $\{F_t\}_{t \geq 0}$ is defined as the σ - algebra generated by all historical data up to the t batch. Specifically, we define the filtration

$$F_t = \sigma(S_1^1, \dots, S_{n_1}^1, S_{n_1+1}^1, \dots, S_1^t, \dots, S_{n_t}^t, S_{n_t+1}^t) \quad (13)$$

For all $t \geq 0$, the sequence of random variables $\{M_t\}_{t \geq 0}$ is defined as:

$$M_t = \max\{(1 - \gamma)E_t^{m\text{-true}} + \gamma M_{t-1}, 1\} \quad (14)$$

where

$$E_t^{m\text{-true}} = \frac{(n_t + 1) \times s_{n_t+1}^{m\text{-true}}}{\sum_{i=1}^{n_t} s_i + s_{n_t+1}^{m\text{-true}}} \quad (15)$$

We will prove that $\{M_t\}_{t \geq 0}$ is a non - negative test supermartingale.

- **Initial condition:** First, we define $M_0 = 1$. Since the non - conformity scores we calculate are positive, it is obvious that for all $t \geq 0$, $M_t \geq 0$. The remaining task is to prove that $\{M_t\}_{t \geq 0}$ is a supermartingale. A non-negative test supermartingale needs to satisfy: $M_0 = 1$ (already satisfied), $M_t \geq 0$ and is F_t - measurable, and $E[M_t|F_{t-1}] \leq M_{t-1}$.
- **Measurability:** To determine whether M_t is measurable after defining the filtration, we use mathematical induction. When $t = 0$, $M_0 = 1$. Since a constant function is measurable with respect to any σ - algebra, M_0 is F_0 - measurable, where $F_0 = \{\emptyset, \Omega\}$ is the trivial σ - algebra. Assume that M_{t-1} is F_{t-1} - measurable. Because $F_{t-1} \subseteq F_t$, M_{t-1} is also F_t - measurable. For the t batch, E_t^{m-true} only depends on the non-conformity scores $S_1^t, \dots, S_{n_t}^t, S_{n_t+1}^t$ of the t - th batch, and these scores are all in F_t , so E_t^{m-true} is F_t - measurable. According to the update rule, let $Z_t = (1 - \gamma)E_t^{m-true} + \gamma M_{t-1}$. Since E_t^{m-true} and M_{t-1} are both F_t - measurable, the linear combination Z_t is also F_t - measurable. Let $A_t = \{\omega \in \Omega : Z_t(\omega) < 1\}$. Since Z_t is F_t - measurable, $A_t \in F_t$. We can rewrite M_t as $M_t = 1 \cdot I_{A_t} + Z_t \cdot I_{A_t^c}$, where I_{A_t} is the indicator function of the set A_t . The indicator functions I_{A_t} and $I_{A_t^c}$ are both F_t - measurable, and the products of the constant 1 and the measurable function Z_t with the indicator functions are also F_t - measurable. Thus, their sum M_t is F_t - measurable. In conclusion, by mathematical induction, we have proved that for the defined filtration $\{F_t\}_{t \geq 0}$, M_t is F_t - measurable.
- **Decreasing conditional expectation:** Under the assumption of within - batch data exchangeability, $E[E_t^{m-true}|F_{t-1}] = 1$. Then the conditional expectation of the supermartingale is

$$E[M_t|F_{t-1}] = (1 - \lambda)E[E_t^{m-true}|F_{t-1}] + \lambda M_{t-1} = (1 - \lambda) + \lambda M_{t-1} \quad (16)$$

Since $M_{t-1} \geq 1$ and $\lambda \in (0, 1)$, we have $E[M_t|F_{t-1}] \leq M_{t-1}$, which satisfies the property of a supermartingale.

Ville's inequality states that for a non - negative supermartingale M_t , $P(\forall t \geq 0, M_t < \frac{1}{\alpha}) \geq 1 - \alpha$. The construction rule of the prediction set is to include the corresponding category in the prediction set when $M_t < \frac{1}{\alpha}$. This means that the probability that the true label falls into the prediction set is at least $1 - \alpha$, thus theoretically guaranteeing the coverage rate of the prediction set. Let x_t be the t - th test sample and Y be the set of all possible categories. For the test sample x_t , its prediction set $\hat{C}(x_t)$ can be expressed as:

$$\hat{C}(x_t) = \left\{ c \in Y : \max\left\{ (1 - \gamma) \frac{(n_t + 1) \cdot s(x_t, c)}{\sum_{i=1}^{n_t} s(x_t, y_i) + s(x_t, c)} + \gamma M_{t-1}, 1 \right\} < \frac{1}{\alpha} \right\} \quad (17)$$

4 Experiments

4.1 Experimental Settings

4.1.1 Datasets

This study conducts model training and evaluation based on two multimodal emotion datasets, IEMOCAP and TESS. The IEMOCAP dataset contains 12 hours of audio-visual data collected across 5 recording sessions, where ten professional actors (5 male, 5 female) simulate real-life interaction scenarios. [Busso et al. \[2008\]](#) For model training, six emotion categories are selected: "ang" (anger), "hap" (happiness), "exc" (excitement), "sad" (sadness), "fru" (frustration), and "neu" (neutral). A stratified sampling approach is employed to ensure each category provides 2,000 balanced training samples. The TESS dataset comprises 2,800 audio files, in which two female actors express seven discrete emotions through the fixed carrier sentence structure "Say the word_". [Pichora-Fuller and Dupuis \[2020\]](#) To establish cross-dataset consistency, only emotion categories overlapping with IEMOCAP are retained. Specifically, "Anger", "Happiness", "Sadness", and "Neutral" in TESS are mapped to the corresponding IEMOCAP labels "ang", "hap", "sad", and "neu", respectively. This label harmonization ensures uniform emotional category definitions during model training and evaluation across datasets.

4.1.2 Base Models

In this study, we used several convolutional neural network (CNN) architectures, including basic CNN, ResNet, MobileNetV3, ShuffleNetV2, SqueezeNet, and GhostNet. We ensured that the number of parameters of these models was similar: ResNet (1,168,955 parameters), MobileNetV3 (1,172,034 parameters), ShuffleNetV2 (1,177,898 parameters), SqueezeNet (1,177,662 parameters), and GhostNet (1,181,503 parameters). These models optimize computational

Algorithm 1 Adaptive Non-Conformal Prediction with Supermartingale (ANCP-S)**Require:**Pre-trained classifier $f : \mathcal{X} \rightarrow \Delta^{K-1}$ Significance level $\alpha \in (0, 1)$ Mixing rate $\gamma \in (0, 1)$ 1: **Initialize**Supermartingale $M_0 \leftarrow 1$ 2: **procedure** ONLINEPREDICTION(Test stream $\{(x_t, y_t)\}_{t=1}^T, \mathcal{D}_{\text{cal}}$)3: **for** $t = 1$ **to** T **do**4: Sample $\mathcal{B}_t \subset \mathcal{D}_{\text{cal}}$ with $|\mathcal{B}_t| = 5$ 5: $\mathbf{p}_t \leftarrow f(x_t)$ $\triangleright \mathbf{p}_t \in \Delta^{K-1}$ 6: Compute $\{s_i\}_{i=1}^n$ where $s_i = 1 - \mathbf{p}_{z_i}(y_i) \forall z_i \in \mathcal{B}_t$ 7: $C_t \leftarrow \emptyset$ 8: **for** $m = 1$ **to** K **do**9: $s_t^m \leftarrow 1 - \mathbf{p}_t(m)$ 10: $E_t^m \leftarrow \frac{(n+1)s_t^m}{\sum_{s_i \in \mathcal{B}_t} s_i + s_t^m}$ 11: $M_t^m \leftarrow \max \{ (1 - \gamma)E_t^m + \gamma M_{t-1}, 1 \}$ 12: **if** $M_t^m < 1/\alpha$ **then**13: $C_t \leftarrow C_t \cup \{m\}$ 14: **end if**15: **end for**16: $E_t^{y_t} \leftarrow \frac{(n+1)(1 - \mathbf{p}_t(y_t))}{\sum_{s_i \in \mathcal{B}_t} s_i + (1 - \mathbf{p}_t(y_t))}$ 17: $M_t \leftarrow \max \{ (1 - \gamma)E_t^{y_t} + \gamma M_{t-1}, 1 \}$ 18: **end for**19: **end procedure**

efficiency and performance through different designs. ResNet50 uses residual connections to solve the gradient vanishing problem of deep networks He et al. [2016], MobileNetV3 and ShuffleNetV2 use lightweight designs to adapt to resource - constrained environments Howard et al. [2019], Ma et al. [2018], and SqueezeNet and GhostNet further optimize the number of model parameters and computational complexity, making them suitable for embedded and mobile device applications. Iandola et al. [2016], Han et al. [2020]

4.1.3 Methods for Speech Feature Extraction

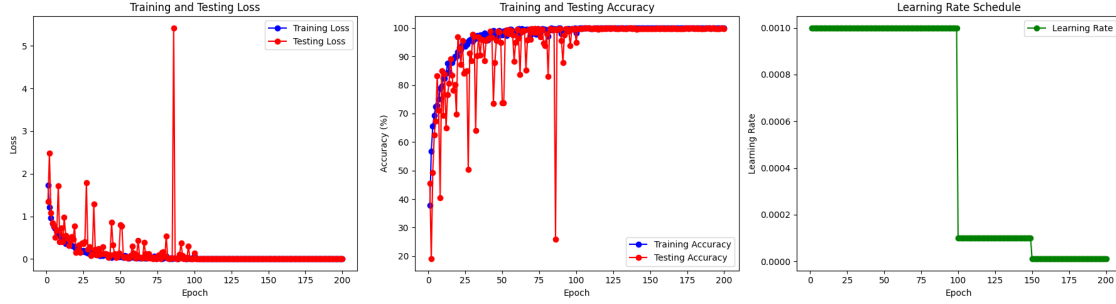
We compared three speech feature extraction methods: Mel spectrogram, chromaticity feature, and contrast feature. Mel spectrogram is a commonly used feature in speech processing. It maps the spectrum of speech signals to the Mel scale, which simulates the human auditory system's ability to perceive different frequencies. By converting the speech signal into a spectrum obtained by short - time Fourier transform (STFT) and applying Mel filter bank processing, Mel spectrogram can effectively extract important frequency components in speech. Compared with traditional linear spectrum, Mel spectrogram can better capture the acoustic characteristics of speech. Chromaticity feature converts spectrum information into energy distribution of 12 scales, representing the change of pitch. Through these features, the tonality information in speech can be reflected, which is particularly important for emotion recognition because different emotions may affect the pitch and tonality of speech. Contrast feature reflects the energy difference between different frequency bands in the spectrum and can describe the local structure of the spectrum. It helps capture the detailed changes in speech by calculating the energy difference between each frequency band and the energy of adjacent frequency bands. It can reflect the emotional color and emotional intensity changes of speech.

4.1.4 Evaluation Metrics

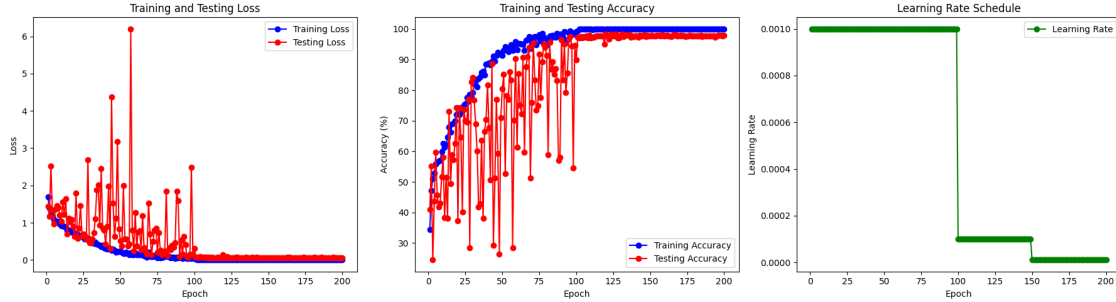
We employ the Empirical Coverage Rate (ECR) to evaluate whether we rigorously control the error rates at various user - specified risk levels. Moreover, we leverage the Average Prediction Set Size to assess the uncertainty of the model's decision - making and the prediction efficiency of the calibrated prediction sets.

4.1.5 Hyper - parameters

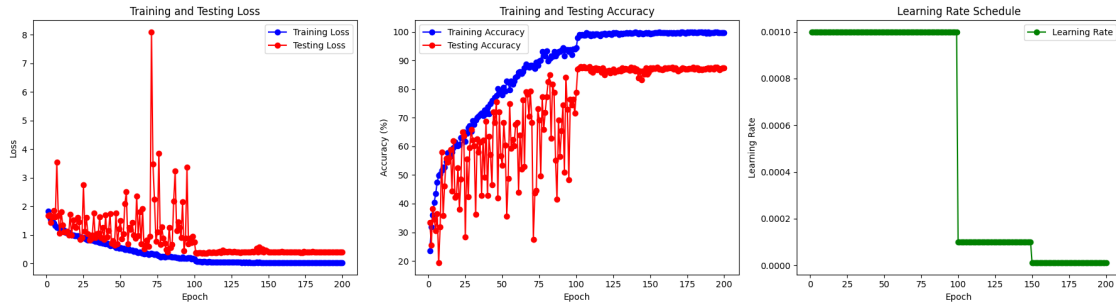
We set the split ratio between the calibration set and the test set to 50% in the IEMOCAP dataset and 50% in the TESS dataset. We modified the structure of the models to ensure that each model has a similar number of parameters: ResNet



(a) Training and testing results of Mel-spectrogram features in basic CNN model



(b) Training and testing results of chromaticity features in the basic CNN model



(c) Training and testing results of contrast features in the basic CNN model

Figure 2: Comparative analysis of the performance of different speech features in basic CNN models based on the TESS dataset

(1,168,955 parameters), MobileNetV3 (1,172,034 parameters), ShuffleNetV2 (1,177,898 parameters), SqueezeNet (1,177,662 parameters), and GhostNet (1,181,503 parameters) to evaluate the uncertainty of different models with the same parameter size.

4.2 Determination of Speech Feature Extraction Methods

In the pre - experimental stage, we compared different speech feature extraction methods, including mel - spectrogram features, chromaticity features, and contrast features. We tested the TESS dataset and found that the accuracy of the mel - spectrogram feature on the test set reached 99.82%[2a](#), significantly better than the chromaticity feature (97.86%)[2b](#) and contrast feature (87.41%)[2c](#). Based on these results, the mel - spectrogram feature showed stronger recognition ability and robustness, so we chose the mel - spectrogram as the optimal feature extraction method and widely used it in the training and evaluation of all models in subsequent experiments.

We trained five models (ResNet, MobileNetV3, ShuffleNetV2, SqueezeNet, and GhostNet), all with a similar number of parameters. During training, mel - spectrogram features were used and trained on the IEMOCAP dataset (60% training set, 40% test set). All models achieved nearly 100% accuracy on the training set, but performed differently on the test set. Specifically, the test set accuracy of ResNet was 41.60%[3a](#), MobileNetV3 was 31.94%[3b](#), ShuffleNetV2 was 34.13%[3c](#), SqueezeNet was 43.46%[3d](#), and GhostNet was 33.40%[3e](#). These results show that although the models performed well

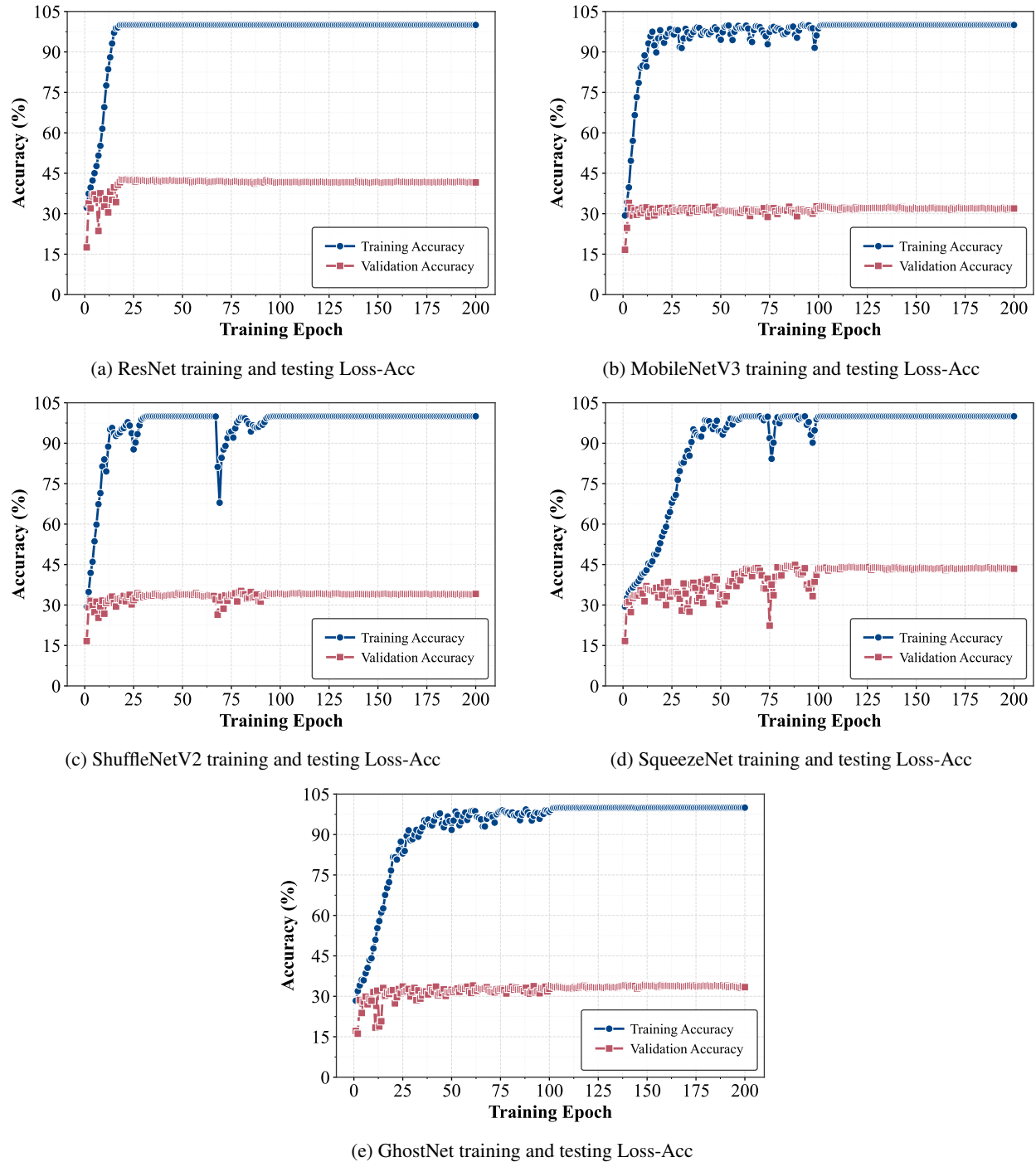


Figure 3: Comparison of training and test set Loss-Acc of different neural network models

on the training set, they had weak generalization ability on the test set, reflecting the overfitting phenomenon, which provides a basis for the subsequent use of the Conformal Prediction framework for model evaluation.

4.3 Empirical Results of the ECR metric

We used SCP and Risk Control frameworks to evaluate the coverage performance of five models on the IEMOCAP dataset, and applied these models to the TESS dataset for testing. On the IEMOCAP and TESS datasets, both

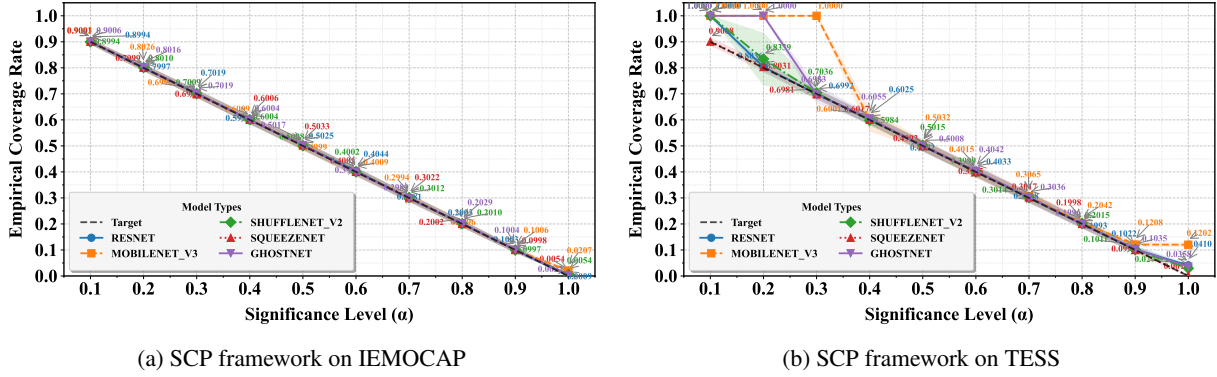


Figure 4: ECR using SCP framework

frameworks provided reliable coverage guarantees and showed that the two frameworks had good generalization capabilities across different datasets Figs. 4 and 5.

While the theoretical guarantee of conformal prediction is rigorous, there can be minor fluctuations in practice due to finite - sample variability.

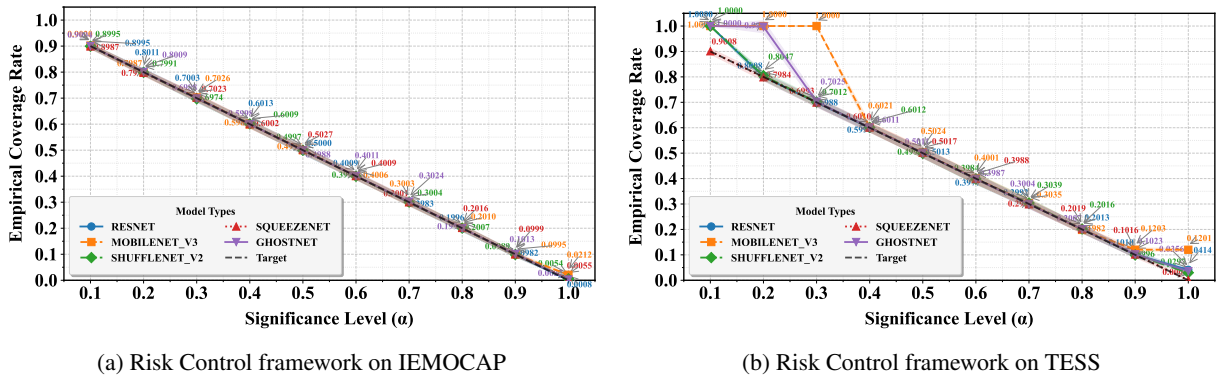


Figure 5: ECR using Risk Control framework

4.4 Uncertainty Estimation of the Model through the APSS metric

We found a negative correlation between the average prediction set size (APSS) and the risk level. Specifically, as the risk level increases, the APSS value decreases significantly¹, indicating that the model’s prediction results at high risk levels are more certain and the size of the prediction set is optimized. In this way, APSS is able to effectively evaluate the uncertainty of the classification model on the test set. Larger APSS values indicate that the model has higher prediction uncertainty for certain categories, while smaller APSS values mean that the model has higher confidence in its predictions. Therefore, APSS, as a measure of model uncertainty, demonstrates its potential as a promising benchmark in evaluating the robustness of classification models and provides a valuable reference for further optimizing models.

4.5 Ablation Studies

This study systematically explores the impact of different data partitioning strategies on model coverage and verifies the robustness of the speech emotion recognition method based on the conformal prediction framework. In the experimental design, we adopt a dynamic calibration mechanism: the confidence threshold q is calculated through the calibration set data, and its statistical validity is verified under different calibration set - test set partition ratios (10%–90%).

The experimental results show that although the calibration set size changes significantly (from 10% to 90%), this method always ensures the empirical coverage of the test set satisfies the theoretical lower bound $1 - \alpha$ ($\alpha = 0.2$)⁶ by dynamically adjusting the confidence threshold q . Theoretical analysis and empirical results jointly prove that this

Table 1: The prediction efficiency of five IEMOCAP-trained models was quantified through Split Conformal Prediction and risk control, measuring average prediction set size (\pm SD) across two evaluation corpora (label counts specified parenthetically).

Dataset	Model	Risk Level								
		0.1	0.2	0.3	0.4	0.5	0.6	0.7	0.8	0.9
Method: Split Conformal Prediction										
IEMOCAP(6)	Resnet	4.025 \pm 0.049	3.106 \pm 0.050	2.319 \pm 0.044	1.755 \pm 0.040	1.297 \pm 0.030	0.941 \pm 0.025	0.621 \pm 0.023	0.362 \pm 0.019	0.160 \pm 0.011
	Mobilenetv3	4.570 \pm 0.062	3.705 \pm 0.063	2.948 \pm 0.052	2.346 \pm 0.064	1.818 \pm 0.040	1.344 \pm 0.035	0.922 \pm 0.026	0.529 \pm 0.027	0.217 \pm 0.015
	Shufflenetv2	4.468 \pm 0.065	3.534 \pm 0.048	2.800 \pm 0.053	2.236 \pm 0.047	1.720 \pm 0.041	1.252 \pm 0.028	0.832 \pm 0.032	0.494 \pm 0.022	0.211 \pm 0.016
	Squeezenet	3.975 \pm 0.072	2.989 \pm 0.051	2.230 \pm 0.048	1.659 \pm 0.044	1.237 \pm 0.031	0.868 \pm 0.021	0.576 \pm 0.025	0.342 \pm 0.017	0.147 \pm 0.011
	Ghostnet	4.657 \pm 0.064	3.698 \pm 0.065	2.973 \pm 0.052	2.319 \pm 0.052	1.761 \pm 0.037	1.276 \pm 0.028	0.855 \pm 0.027	0.519 \pm 0.020	0.235 \pm 0.016
TESS(4)	Resnet	4.000 \pm 0.000	2.893 \pm 0.059	2.551 \pm 0.035	2.230 \pm 0.041	1.894 \pm 0.044	1.580 \pm 0.040	1.225 \pm 0.029	0.663 \pm 0.120	0.191 \pm 0.017
	Mobilenetv3	4.000 \pm 0.000	4.000 \pm 0.000	4.000 \pm 0.000	2.210 \pm 0.182	1.846 \pm 0.050	1.526 \pm 0.039	1.161 \pm 0.047	0.662 \pm 0.056	0.281 \pm 0.008
	Shufflenetv2	4.000 \pm 0.000	3.106 \pm 0.558	2.490 \pm 0.051	2.161 \pm 0.047	1.819 \pm 0.042	1.480 \pm 0.038	1.125 \pm 0.034	0.626 \pm 0.047	0.199 \pm 0.022
	Squeezenet	3.621 \pm 0.051	3.190 \pm 0.055	2.751 \pm 0.060	2.364 \pm 0.064	1.897 \pm 0.056	1.483 \pm 0.059	0.977 \pm 0.045	0.535 \pm 0.042	0.222 \pm 0.018
	Ghostnet	4.000 \pm 0.000	4.000 \pm 0.000	2.439 \pm 0.026	2.176 \pm 0.043	1.873 \pm 0.040	1.562 \pm 0.052	1.216 \pm 0.035	0.695 \pm 0.059	0.255 \pm 0.024
Method: Risk Control										
IEMOCAP(6)	Resnet	4.017 \pm 0.061	3.091 \pm 0.059	2.306 \pm 0.041	1.759 \pm 0.042	1.294 \pm 0.029	0.935 \pm 0.027	0.619 \pm 0.022	0.361 \pm 0.017	0.155 \pm 0.012
	Mobilenetv3	4.574 \pm 0.060	3.691 \pm 0.058	2.951 \pm 0.049	2.333 \pm 0.043	1.828 \pm 0.042	1.340 \pm 0.042	0.922 \pm 0.027	0.532 \pm 0.025	0.215 \pm 0.015
	Shufflenetv2	4.464 \pm 0.064	3.553 \pm 0.054	2.801 \pm 0.054	2.230 \pm 0.048	1.713 \pm 0.045	1.240 \pm 0.032	0.823 \pm 0.029	0.495 \pm 0.024	0.210 \pm 0.016
	Squeezenet	3.964 \pm 0.061	2.979 \pm 0.062	2.217 \pm 0.048	1.666 \pm 0.037	1.234 \pm 0.032	0.868 \pm 0.026	0.569 \pm 0.025	0.344 \pm 0.018	0.149 \pm 0.013
	Ghostnet	4.649 \pm 0.059	3.707 \pm 0.071	2.979 \pm 0.056	2.313 \pm 0.049	1.764 \pm 0.037	1.271 \pm 0.033	0.859 \pm 0.030	0.518 \pm 0.021	0.235 \pm 0.015
TESS(4)	Resnet	4.000 \pm 0.000	2.887 \pm 0.042	2.555 \pm 0.042	2.219 \pm 0.040	1.904 \pm 0.039	1.581 \pm 0.043	1.223 \pm 0.037	0.666 \pm 0.115	0.188 \pm 0.017
	Mobilenetv3	4.000 \pm 0.000	4.000 \pm 0.000	4.000 \pm 0.000	2.214 \pm 0.051	1.849 \pm 0.041	1.513 \pm 0.044	1.158 \pm 0.043	0.649 \pm 0.061	0.280 \pm 0.009
	Shufflenetv2	4.000 \pm 0.000	2.840 \pm 0.047	2.494 \pm 0.048	2.153 \pm 0.039	1.814 \pm 0.040	1.477 \pm 0.039	1.126 \pm 0.033	0.611 \pm 0.044	0.196 \pm 0.023
	Squeezenet	3.613 \pm 0.046	3.192 \pm 0.051	2.751 \pm 0.052	2.359 \pm 0.058	1.921 \pm 0.065	1.477 \pm 0.063	0.978 \pm 0.042	0.530 \pm 0.033	0.221 \pm 0.021
	Ghostnet	4.000 \pm 0.000	3.975 \pm 0.174	2.486 \pm 0.051	2.174 \pm 0.050	1.865 \pm 0.046	1.556 \pm 0.052	1.215 \pm 0.031	0.676 \pm 0.065	0.249 \pm 0.024

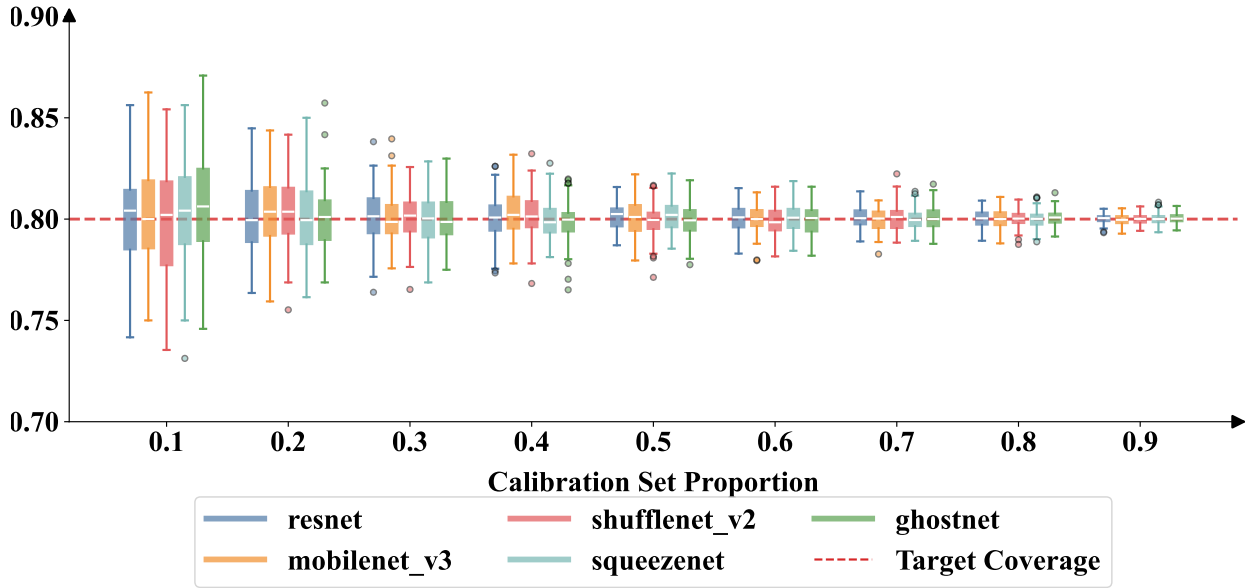


Figure 6: Coverage Distribution vs Calibration Set Size ($\alpha = 0.2$)

method exhibits strong robustness to data partition ratios. The constructed prediction sets provide statistically rigorous reliability guarantees for speech emotion recognition tasks, effectively addressing the confidence calibration failure problem in traditional methods caused by data distribution shifts.

4.6 Relax the exchangeability based on small batch martingale process

In order to verify the effectiveness of the proposed martingale method and the rationality of the assumption of local interchangeability in small batch scenarios, this paper adopts a cross-dataset experimental design, focusing on the actual scenario where inter-batch data does not meet global interchangeability. The calibration set is selected from the

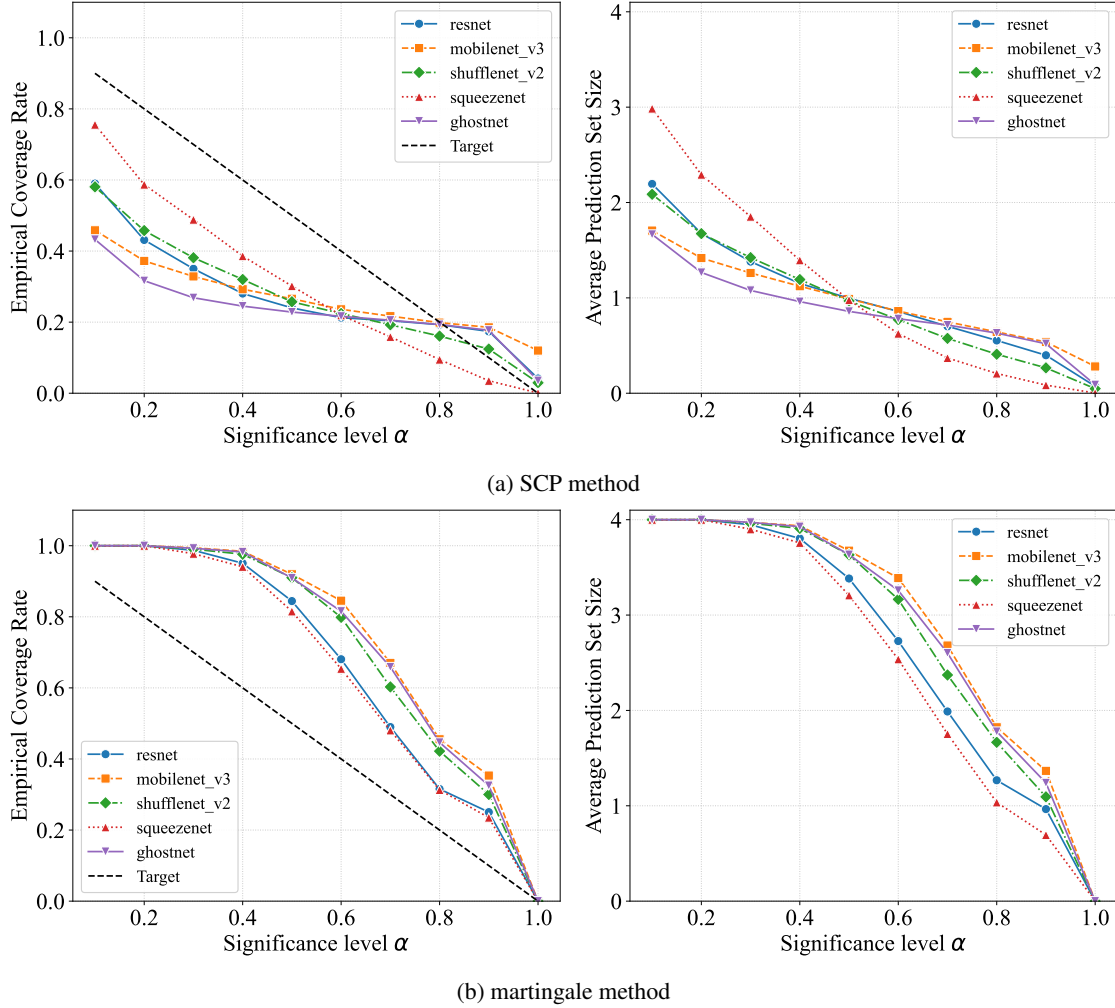


Figure 7: Coverage guarantee based on martingale method

IEMOCAP speech emotion dataset, and the test set is the TESS dataset. There are significant differences in the speaker, emotional expression mode and acoustic environment, forming a typical domain offset problem, which directly leads to inconsistent data distribution between batches (that is, the inter-batch does not meet the interchangeability). The experiment divides the data into "local batches", each batch contains 5 calibration data and 1 test data, strengthening the local correlation of internal data by limiting the batch size - although there may be significant distribution differences between batches (such as grouping characteristics of different time periods and different scenarios), the data within a single batch can approximately meet "local interchangeability" because it comes from a closer local distribution.

As shown in the figure 7, traditional methods experience significant coverage bias when data does not satisfy exchangeability, as the global exchangeability assumption fails, resulting in empirical coverage below the target value. This method uses the local exchangeability assumption and martingale value screening, and when the distribution difference between batches is significant, the empirical coverage rate and target value are still achieved, verifying the validity of the relaxation assumption that "interchangeability can not be met between batches". M_t significantly affects the quality of the conformal set at batch t . As the martingale approaches zero, the conformal set becomes larger and less informative. The figure shows the changing path of M_t . It is worth noting that this method ensures coverage but does not control the size of the conformal set; stronger models generally produce smaller sets.

This framework does not require global data to obey the same distribution, significantly relaxing the prerequisites for traditional conformal prediction, and is suitable for complex scenarios where there is a distribution offset between batches.

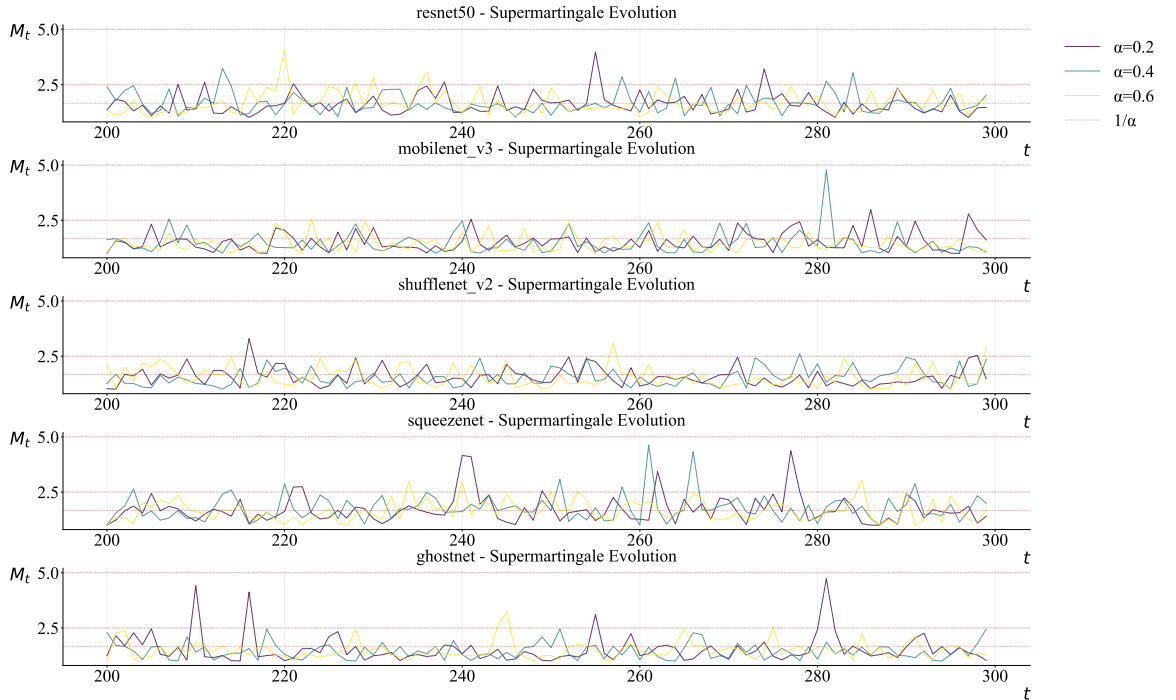


Figure 8: Supermartingale Analysis

5 Conclusion

This study proposes a solution based on CP and risk control framework to solve the problem of unreliable prediction of traditional neural networks in speech emotion recognition. The results show that traditional point prediction methods have significant confidence bias due to factors such as data distribution differences, model overfitting, and difficulty in capturing complex emotional features. By using the SCP framework and risk control framework, this study successfully transforms single-point predictions into set predictions with coverage guarantees, ensuring that the true label is included in the prediction set with a probability of at least $1 - \alpha$ under a specified risk level α . In addition, cross-dataset validation proves the robustness of the framework under different data distributions. The study also finds that APSS is negatively correlated with the risk level, indicating that when the risk level is high, the model’s prediction set is usually smaller and the model’s prediction uncertainty is lower. Based on this finding, we propose a metric for evaluating the uncertainty of classification models on the test set. At the same time, our mini-batch martingale value conformal prediction theory extends the applicability of CP to non-exchangeable environments, solving a key flaw in existing uncertainty quantification methods. By adopting the local exchangeability assumption within the mini-batch and constructing a non-negative test martingale, our method maintains coverage guarantees even under non-IID data distributions.

References

- Apostolos F Psaros, Xuhui Meng, Zongren Zou, Ling Guo, and George Em Karniadakis. Uncertainty quantification in scientific machine learning: Methods, metrics, and comparisons. *Journal of Computational Physics*, 2023.
- Zhiyuan Wang, Jinhao Duan, Chenxi Yuan, Qingyu Chen, Tianlong Chen, Yue Zhang, Ren Wang, Xiaoshuang Shi, and Kaidi Xu. Word-sequence entropy: Towards uncertainty estimation in free-form medical question answering applications and beyond. *Engineering Applications of Artificial Intelligence*, 2025a.
- Anastasios N Angelopoulos and Stephen Bates. A gentle introduction to conformal prediction and distribution-free uncertainty quantification. *arXiv preprint arXiv:2107.07511*, 2021.

- Fanghua Ye, Mingming Yang, Jianhui Pang, Longyue Wang, Derek Wong, Emine Yilmaz, Shuming Shi, and Zhaopeng Tu. Benchmarking llms via uncertainty quantification. *Advances in Neural Information Processing Systems*, 2024.
- Rina Foygel Barber, Emmanuel J. Candes, Aaditya Ramdas, and Ryan J. Tibshirani. Conformal prediction beyond exchangeability. *The Annals of Statistics*, 2023.
- Zhiyuan Wang, Jinhao Duan, Lu Cheng, Yue Zhang, Qingni Wang, Xiaoshuang Shi, Kaidi Xu, Heng Tao Shen, and Xiaofeng Zhu. ConU: Conformal uncertainty in large language models with correctness coverage guarantees. In *Findings of the Association for Computational Linguistics: EMNLP 2024*, 2024.
- Sophia Huiwen Sun and Rose Yu. Copula conformal prediction for multi-step time series prediction. In *The Twelfth International Conference on Learning Representations*, 2023.
- Qingni Wang, Tiantian Geng, Zhiyuan Wang, Teng Wang, Bo Fu, and Feng Zheng. Sample then identify: A general framework for risk control and assessment in multimodal large language models. In *The Thirteenth International Conference on Learning Representations*, 2025b.
- Mintong Kang, Nezihe Merve Gürel, Ning Yu, Dawn Song, and Bo Li. C-rag: Certified generation risks for retrieval-augmented language models. In *ICML*, 2024.
- Zhiyuan Wang, Qingni Wang, Yue Zhang, Tianlong Chen, Xiaofeng Zhu, Xiaoshuang Shi, and Kaidi Xu. SConU: Selective conformal uncertainty in large language models. *arXiv preprint arXiv:2504.14154*, 2025c.
- Etienne Gauthier, Francis Bach, and Michael I Jordan. E-values expand the scope of conformal prediction. *arXiv preprint arXiv:2503.13050*, 2025.
- Carlos Busso, Murtaza Bulut, Chi-Chun Lee, Abe Kazemzadeh, Emily Mower, Samuel Kim, Jeannette N Chang, Sungbok Lee, and Shrikanth S Narayanan. Iemocap: Interactive emotional dyadic motion capture database. *Language resources and evaluation*, 42:335–359, 2008.
- M Kathleen Pichora-Fuller and Kate Dupuis. Toronto emotional speech set (tess)(2020). URL: <https://tspace.library.utoronto.ca/handle/1807/24487>. DOI: <https://doi.org/10.5683/SP2/E8H2MF>, 2020.
- Kaiming He, Xiangyu Zhang, Shaoqing Ren, and Jian Sun. Deep residual learning for image recognition. In *Proceedings of the IEEE conference on computer vision and pattern recognition*, pages 770–778, 2016.
- Andrew Howard, Mark Sandler, Grace Chu, Liang-Chieh Chen, Bo Chen, Mingxing Tan, Weijun Wang, Yukun Zhu, Ruoming Pang, Vijay Vasudevan, et al. Searching for mobilenetv3. In *Proceedings of the IEEE/CVF international conference on computer vision*, pages 1314–1324, 2019.
- Ningning Ma, Xiangyu Zhang, Hai-Tao Zheng, and Jian Sun. Shufflenet v2: Practical guidelines for efficient cnn architecture design. In *Proceedings of the European conference on computer vision (ECCV)*, pages 116–131, 2018.
- Forrest N Iandola, Song Han, Matthew W Moskewicz, Khalid Ashraf, William J Dally, and Kurt Keutzer. Squeezenet: Alexnet-level accuracy with 50x fewer parameters and < 0.5 mb model size. *arXiv preprint arXiv:1602.07360*, 2016.
- Kai Han, Yunhe Wang, Qi Tian, Jianyuan Guo, Chunjing Xu, and Chang Xu. Ghostnet: More features from cheap operations. In *Proceedings of the IEEE/CVF conference on computer vision and pattern recognition*, pages 1580–1589, 2020.